

Experimental study on the behavior of a new post-grouted micropile in a tropical soil

Joaquim Ribeiro Castro Neto¹ , Paulo José Rocha de Albuquerque¹ ,
Yuri Barbosa^{1#} , Luiz Felipe Goulart Fiscina¹ 

Case Study

Keywords

Post-grouted micropiles
Static load tests
Instrumentation
Pile shaft bearing capacity
Tropical soils

Abstract

This work aims to analyze the behavior of a new post-grouted micropile setup developed in tropical soil. Its main innovation is the use of high mechanical resistance steel pipes (N80 class) for drilling and as a structural component of the micropiles. The pipes have special manchette valves uniformly spaced to allow neat cement grout injection into the soil. Two instrumented micropiles with 0.3 m diameter (after injection) and lengths of 19.4 m and 21 m were installed at Experimental Site III of the University of Campinas (Unicamp). The geological profile of this site presents a sandy clay surface layer (porous and collapsible) followed by a layer of sandy silt (diabase residual soil). The piles were subjected to compressive slow maintained loading tests and were instrumented along their depth with strain gages. No geotechnical failure was observed during the load test. The maximum load achieved by the MC1 and MC2 micropiles were 2.210 kN and 2.470 kN, respectively. The load test data were extrapolated to estimate the ultimate geotechnical pile capacity. The extrapolated geotechnical failure load was above 2.500 kN for both micropiles and similar to those estimated by the Federal Highway Administration FHWA (2005) load capacity method. It was verified that (1) the pile material undergoes creep under stress above 25 MPa on the transversal section of the pile and (2) the debonding effect during the loading process. The micropiles showed higher values of skin friction compared with other piles installed in the same geological-geotechnical context (tropical soil).

1. Introduction

The micropile was first conceived in Europe in the 1950s, when Fernando Lizzi developed the pali radice as a foundation technique. The main characteristic of the micropile installation technique is the performance of this type of deep foundation in high-resistance soils (including rocks), spaces with low ceilings and places with uneven surface (FHWA, 2005). Due to the small diameter (typically around 0.3 m) or the difficulty of assuring adequate cleaning of the borehole, tip resistance is generally disregarded and only load transfer by skin friction is considered (Allen et al., 2004). According to Choi & Cho (2010), neat cement grout injection may increase the load capacity of the micropiles by more than 100%, both in soil and rock.

Some authors (Finno et al., 2002; Holman & Barkauskas, 2007) point out that a relative displacement between the steel casing and the neat cement grout may occur. Allen et al. (2004) and Holman & Barkauskas (2007) suggest that this phenomenon, called debonding effect, results from inadequate

preparation of the pile head or from eccentric loads. According to FHWA (2005), the debonding effect may be disregarded, and adhesion between the smooth metal tube and the neat cement grout varies from 1 to 1.75 MPa. Fiscina et al. (2021) conclude that the mobilized skin friction of the soil-micropile interface was 2.4 and 1.7 higher than other types of piles installed in similar underground conditions.

FHWA (2005) classifies micropiles into four types based on the injection technique and on the applied pressure. Table 1 shows these classifications.

Due to its complex behavior, several studies seek to understand the behavior of these deep foundation elements by using numeric tools, analytical models, or load tests. Numerical modeling is a widely employed tool for evaluating the pile load capacity and its load transfer mechanisms (Loukidis & Salgado, 2008; Han et al., 2017; Mendoza et al., 2017; Khanmohammadi & Fakharian, 2019; Ong et al., 2021). Park et al. (2012), Dias & Bezuijen (2018) and Kim et al. (2020) achieved acceptable results evaluating the load transfer mechanism of piles by using analytical

[#]Corresponding author. E-mail address: ybarbosa39@gmail.com

¹Universidade Estadual de Campinas, School of Civil Engineering, Architecture and Urban Design, Campinas, SP, Brasil.

Submitted on May 25, 2022; Final Acceptance on October 10, 2022; Discussion open until February 28, 2023.

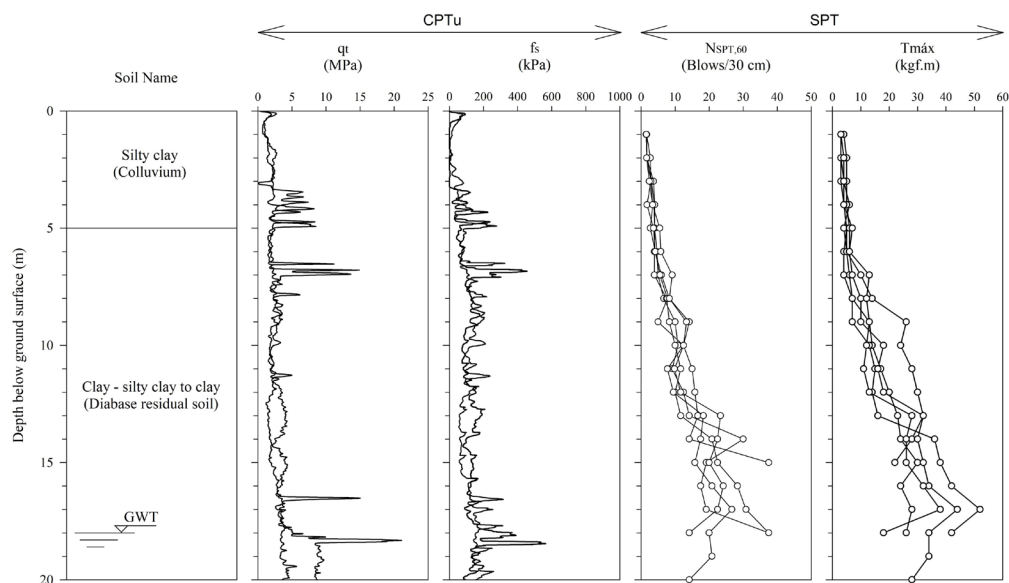
<https://doi.org/10.28927/SR.2022.005322>



This is an Open Access article distributed under the terms of the Creative Commons Attribution License, which permits unrestricted use, distribution, and reproduction in any medium, provided the original work is properly cited.

Table 1. Micropile classification (FHWA, 2005).

Type of micropile	Description
Type A	Neat cement grout is tremied into the borehole. It does not use pressure grouting injection (Gravity Fill Technique).
Type B	Pressure grouting injection during withdrawal of the steel casing (0.5 to 1 MPa).
Type C IGU	First, the borehole is filled with neat cement grout. Then, neat cement grout is pressure injected from the head of the pile through a tube with valves (Post-grouting technique with pressures above 1 MPa).
Type D IRS	First, the annulus sheath is formed with neat cement grout via a single packer. Afterwards, neat cement grout is pressure injected, locally, via a double packer (pressures up to 2 MPa). The injection phases are usually spaced 24 hours apart and the process may be repeated up to four times. Lastly the borehole is filled with neat cement grout.


Figure 1. Physical and mechanical properties of the layered soil at ESIII.

models with emphasis in the discrete formulations, which considers different properties along the depth of the pile. Load tests are widely employed to understand the behavior of the piles and to validate computational tools and empirical and semiempirical calculation methodologies (Russo, 2004; Ko et al., 2018; Wan et al., 2019; Fattah et al., 2020; Freitas Neto et al., 2020).

Several papers evaluate the accuracy of empirical or semiempirical methods by using the results of load tests as a validation technique. In general, they suggest correction parameters to adjust the geotechnical characteristics of the subsoil conditions and the mechanical properties of the piles (Titi & Abu-Farsakh, 1999; Décourt, 2008; Niazi & Mayne, 2013; Wrana, 2015; Ebrahimian & Movahed, 2017; Eid et al., 2018; Moshfeghi & Eslami, 2018; Song et al., 2020; Jeong et al., 2021). Some methods were developed specifically for micropiles, such as: Bustamante & Doix (1985), Lizzi (1985) and FHWA (2005). Thereby, this study aims to present a new micropile technique in Brazil, evaluate its performance in a tropical soil by using instrumented load

tests and compare its results with other piles installed in the same geological-geotechnical context.

2. Geological and geotechnical site characteristics

The load tests were performed at the Experimental Site III (ES III) of the University of Campinas, located in the city of Campinas, in the state of São Paulo, Brazil. Information on the site is provided in Albuquerque (2001), Castro Neto (2021), Fiscina (2020), and Fiscina et al. (2021).

Figure 1 shows the N_{SPT} , q_t , and f_s variation graphs based on five Standard Penetrations Tests (SPT) and two Piezocone Penetration Tests (CPTu). The upper layer is composed of porous silty clay (colluvial soil) about 5 m in depth, followed by ~25 m of silty clay (diabase residual soil). Lateritic concretion lenses of around 0.5 m were observed at a depth of 7 m. Such material can be identified in the peak values provided by the CPTu (q_t and f_s) along the test depth. Finally, the groundwater table (GWT) was found at a depth of 18 m.

Figure 2 shows the average geotechnical characteristics of the soil layers and the total length of the piles after their installation. The piles had a post-injection diameter of 0.3 m and lengths of 21 m (MC1) and 19.4 m (MC2). Both were installed according to the Type D methodology conforming to FHWA (2005). However, only the MC1 micropile had its manchette valves opened during the construction process.

3. Experimental set-up

The micropile in the present study is the result of a new construction technique that employs a special steel tube ($\phi = 200$ mm - API N-80) with four main functionalities: drilling tool, casing protection, injection device (manchette valves system installed on the steel tube surface), and structural element. A brief description of the construction technique is presented below:

- a) The first step is drilling by roto-percussion and water circulation using segments of steel tubes with threads. The initial segment has a drilling crown (Figure 3a) to facilitate cutting the soil. Tricone or eccentric bits with diamond or widia components can be used in case of more resistant bearing strata;
- b) Then, a single packer (Figure 3b) is inserted inside the tube, at the tip of the micropile. Neat cement grout is injected with an ascending flux to fill the annulus space between the tube and the soil, constituting the annulus sheath, and removing any residual debris from drilling;
- c) After the cure of the annulus sheath, a double packer (Figure 3c) is inserted for the post-grouting treatment. It is positioned at predetermined locations (starting from deeper positions), with the procedure being carried out from the bottom up. Note that the pressure injection can be carried out more than

once – 1st phase, 2nd phase etc. – depending on the project/geotechnical consultant specifications;

- d) Lastly, the steel tube is filled with neat cement grout from the bottom up. Figure 4 shows all phases of the construction process.

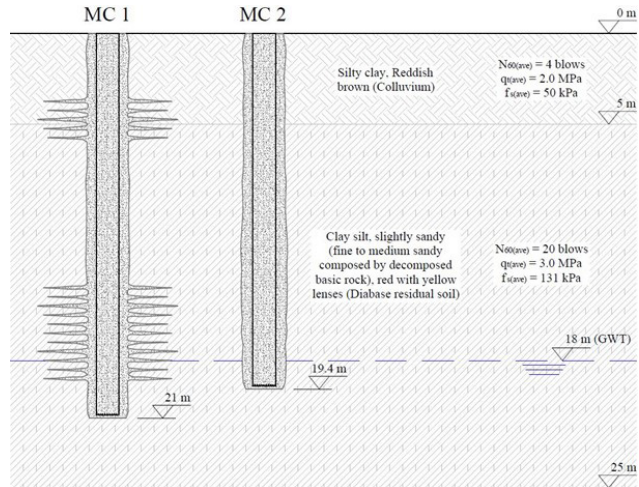


Figure 2. Estimated geotechnical profile of Experimental Site III.

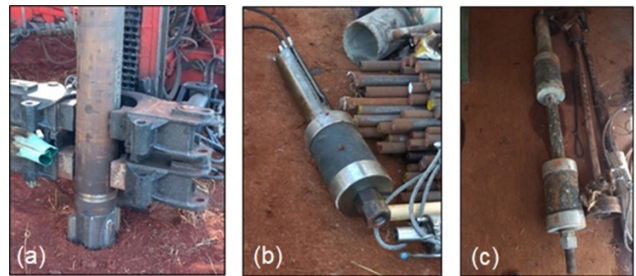


Figure 3. Tools used for the micropile construction: (a) tube coupled to the drill, (b) single packer and (c) double packer.

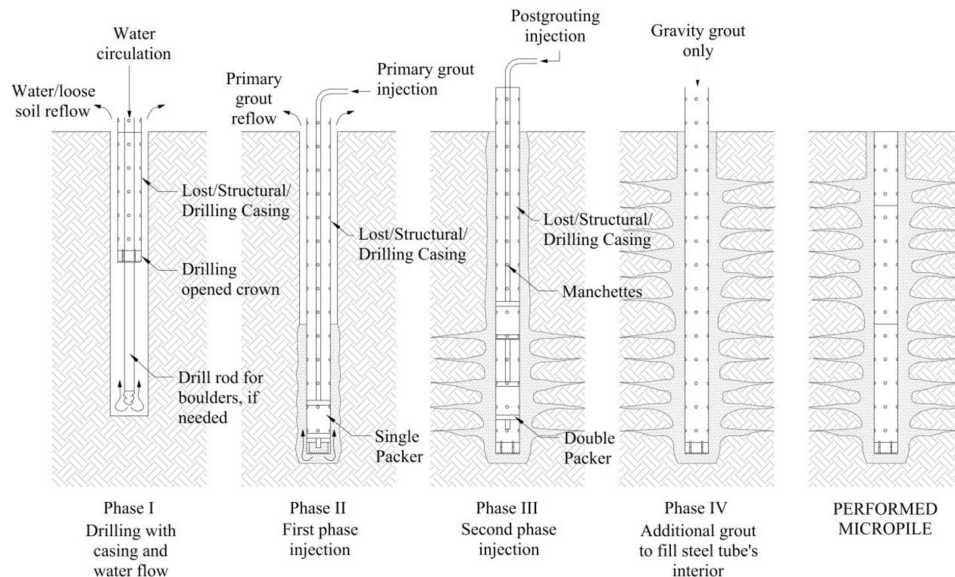


Figure 4. Micropile construction phases (Fiscina et al., 2021).

It is worthy to state that the manchette valves are previously installed in the walls of the steel tubes, in groups of four, diametrically opposed and vertically spaced by 0.5 m (industrial process). They have an aluminum body and a rubber packer, which opens with pressures up to 2 MPa, approximately (Figure 5). They close immediately after the pressure is released, preventing the neat cement grout from flowing back into the steel tube. To assure the correct operation of the device, the neat cement grout must have a cement-water factor of 0.5.

The instrumentation of the micropiles was performed using strain gages previously installed in steel bars of 12.5 mm in diameter and 0.5 m in length (instrumented bars). They were inserted after the post-grouting treatment (between Phase III and IV – Figure 4). Figure 6 shows the position of the instrumented bars alongside the pile depth, highlighting

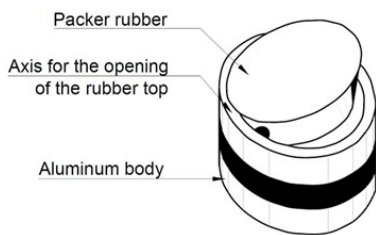


Figure 5. Neat cement grout injection valve.

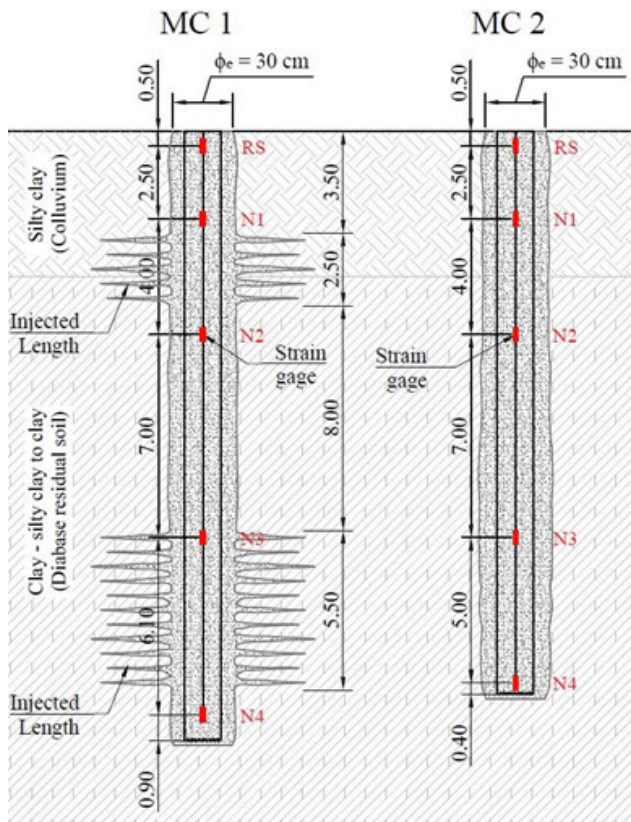


Figure 6. Instrumentation levels.

the MC1’s manchette valves which opened after receiving the post-grouting treatment. Post-grouting injections were not performed for MC2 pile.

The reaction system of the load tests was designed to apply a maximum load of 3000 kN. It was composed of four reaction micropiles, a steel double I-beam, a hydraulic jack and a load cell (Figure 7). The static load-maintained test (SLMT) was conducted according to the instructions of the Brazilian Standard ABNT NBR 12131 (ABNT, 2006) with load increments of 130 kN.

4. Analysis and results

Figure 8 shows the load vs movement curve of the micropiles studied. The MC1 reached a maximum load of 2210 kN with a movement of 24 mm while the MC2 reached a load of 2470 kN and a movement of 26 mm. The SMLT for MC1 was paralyzed due to a sudden failure of the pile cap/pile system, similar experience was evidenced by Fiscina et al. (2021). For MC2, the movement evolved continuously with

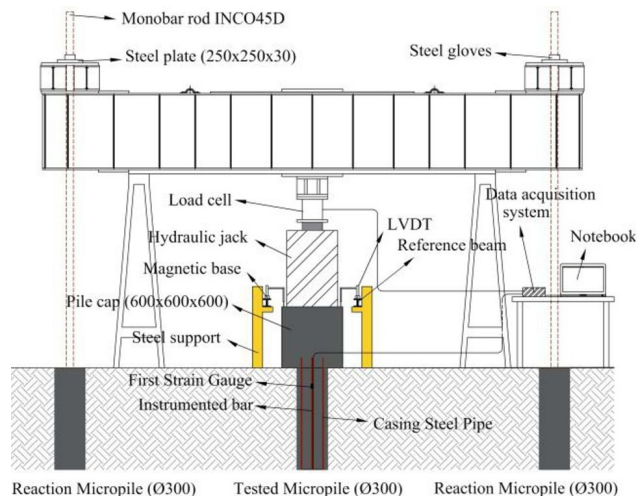


Figure 7. Load test assembly scheme (adapted from Fiscina et al., 2021).

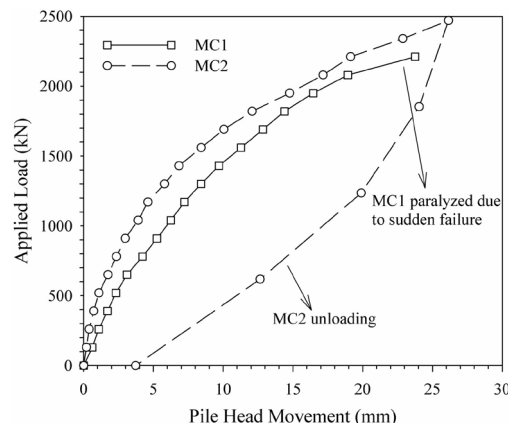


Figure 8. Load-displacement curves for micropiles.

the increase of the load without characterizing a conventional failure (close to 10% pile diameter). The test was stopped due to excessive deformation of the reaction system.

Since the results do not characterize a geotechnical failure, the Van der Veen (1953) method modified by Aoki (1976) was employed to extrapolate the data results, which resulted in an ultimate load capacity of 2560 kN and 2764 kN for the MC1 and MC2 micropiles, respectively. The ultimate load capacity was also estimated by the Bustamante & Doix (1985), Lizzi (1985) and FHWA (2005) semiempirical methods. Table 2 shows the results obtained by those methods.

Figure 9 presents the ratio of the estimated values for ultimate load capacity to the experimental ultimate load capacity obtained via SMLT. The FHWA (2005) and Lizzi (1985) methods showed similar results for both micropiles. This did not occur for the Bustamante & Doix (1985) method, which considers the initial annulus sheath volume and the post-grouting phases. Moreover, the Bustamante & Doix (1985) method also considers the tip resistance in the overall pile capacity calculation while the FHWA (2005) and Lizzi (1985) methods do not take it into account. The FHWA (2005) method showed results in the range of $\pm 20\%$ of the variation which indicates to be a fit model to predict the geotechnical capacity of these types of piles embedded in tropical soil.

Figure 10 shows the load vs deformation curves along the micropile depth. The reference section exhibits deformations with an elastic behavior up to 1800 kN (25 MPa stress at the cross-section area, approximately), manifesting a creep

response from this load up. Note that the MC2 micropile showed an unexpected behavior at level N2, with progressive stiffness loss after the tenth stage load.

The pile stiffness was obtained using the Incremental Stiffness Method (Fellenius, 1989; Fellenius, 2021) modified by Komurka & Moghaddam (2020). The tangential stiffness vs strain graphs (Figure 11) had a linear trend after 500 $\mu\epsilon$, indicating that the skin friction was fully mobilized for the three upper levels (SR, N1, and N2). According to Fellenius (1989, 2001, 2021), after the graph converges to a straight line, the deep foundation element has the mechanical behavior of a column, so the calculated deformation module does not suffer interference from the surrounding soil. Therefore, considering the micropile diameter as 0.3 m, the deformation module of the micropiles is approximately equal to 11 GPa and 16 GPa for MC1 and MC2, respectively. These values are inferior to those of concrete piles, which are, in general, around 20 to 25 GPa (Albuquerque, 2001; Albuquerque et al., 2007, 2014). This can be explained by the fact that the neat cement grout does not use aggregates in its composition, which reduces the overall pile stiffness (Laister et al., 2014).

Table 2. Ultimate load capacity of the micropiles.

Method	MC1(in kN)	MC2(in kN)
FHWA (2005)	2555	2339
Lizzi (1985)	2227	2000
Bustamante & Doix (1985)	5518	4920

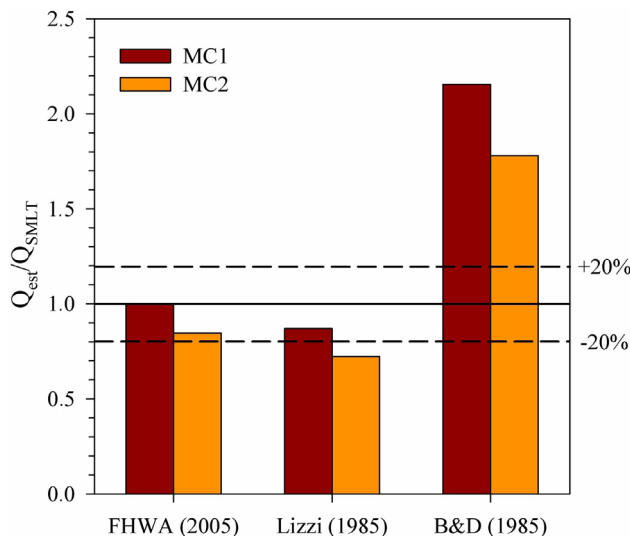


Figure 9. Comparison of estimated results.

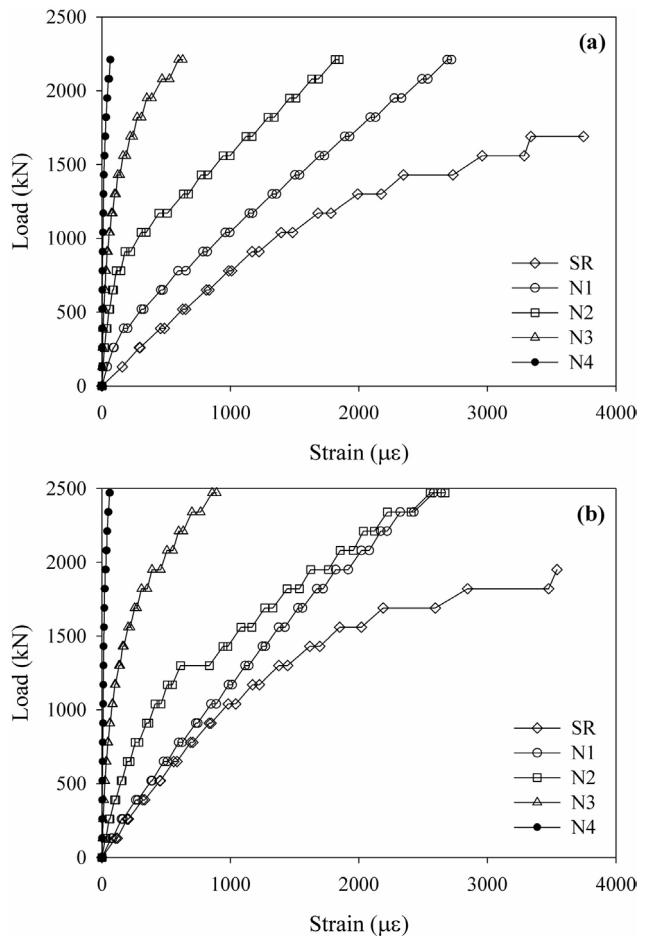


Figure 10. Load vs deformation graphs for micropiles (a) MC1 and (b) MC2.

Figure 12a shows the load transfer along the depth of the MC1 micropile. It indicates a linear behavior after 1820 kN and constant skin friction up to 14 m of depth. According to Figure 12b, the micropile MC2 presented a variation of the load transfer mechanism after the load stage of 1170 kN (between 3.0 and 7.0 m), which indicates a loss of friction in that region. The load transfer in the soil/

micropile interface is progressively reduced until reaching a constant value at the last load stage, i.e., at this region there is no load transfer from the pile to the soil. This is probably due to excessive fissuring of the neat cement grout, which may have compromised the adhesion between the pile and the surrounding soil. According to Gomez et al. (2003) and Fiscina et al. (2021), this phenomenon is called debonding effect and happens when the pile-soil interface is unable to retain significant shear resistance. It is worth mentioning that the strength values of the neat cement grout at 28 days used in the present study (approximately equal to 15MPa) were below the values recommended by the FHWA (2005), which vary between 28 MPa to 35 MPa. The maximum tip load was 63 kN and 75 kN for MC1 and MC2, respectively, which in terms of the overall pile capacity is negligible.

Figure 13a shows that the maximum mobilized skin friction on the MC1 micropile was in the region treated with neat cement grout (3 m to 7 m from the top of the pile), reaching a value equal to 150 kPa (last load stage). In addition, the weighted average skin friction along the micropiles depth was equal to 112 kPa (last load stage). For the MC2 micropile, the highest mobilized skin friction value was 222 kPa, in the region from 7 m to 14 m from the top of the pile (Figure 13b). At the last load stage, the weighted average skin friction along the length of the micropile was 137 kPa, showing that the post-grouting treatment with high pressures does not necessarily guarantee the increasing of the skin friction of the micropile.

Figure 14 presents that the development of the unit skin friction (average value) with the displacement of the shaft follows the same trend for both piles, as verified by the B parameter (MC1 = 32 kPa/mm and MC2 = 38 kPa/mm). Also, the displacements for mobilizing the maximum skin friction were around 1.2% and 0.7% of the pile diameter for the MC1 and MC2 micropiles, respectively. These values are in accordance with the findings of Albuquerque (2001), Wada (2004) and Meyer & Żarkiewicz (2018).

Figure 15 shows the stiffness trend of current post-grouted micropile compared with other types performed at the Experimental Site I (Albuquerque, 2001; Albuquerque et al.,

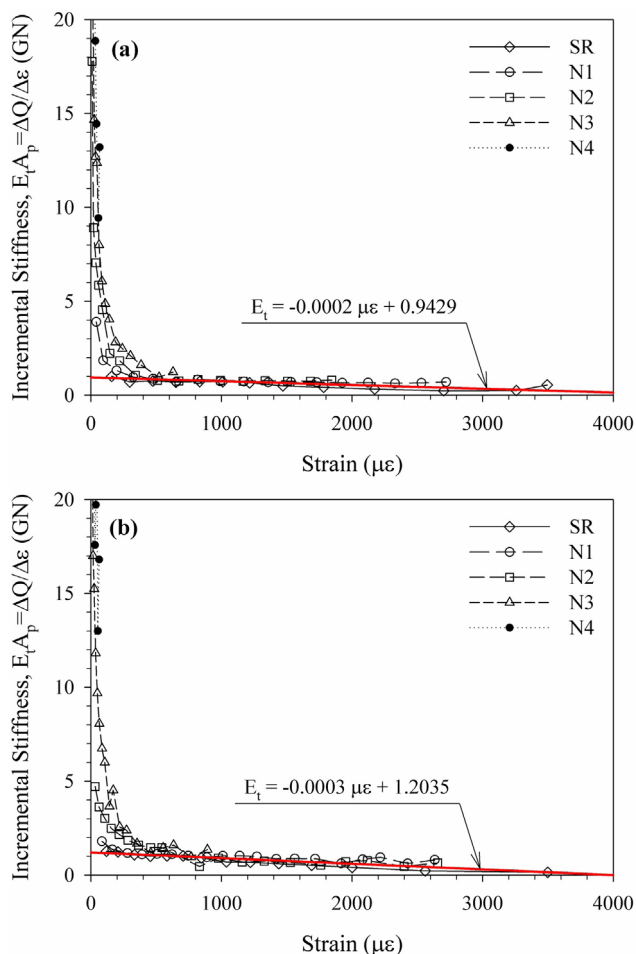


Figure 11. Incremental stiffness vs strain graphs for micropiles (a) MC1 and (b) MC2.

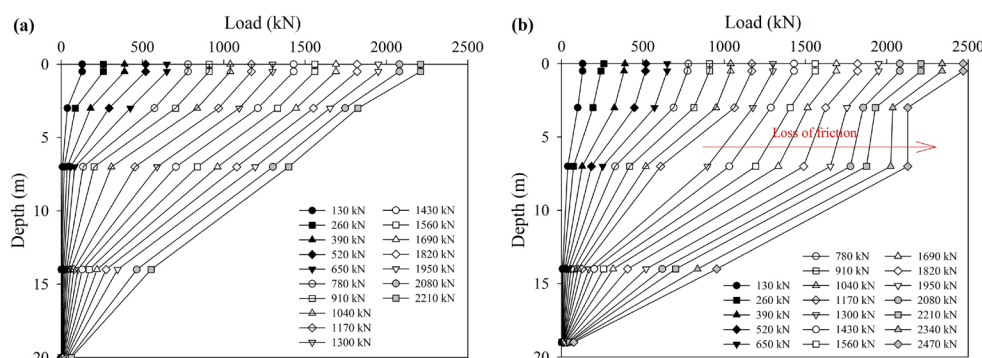


Figure 12. Load transfer for micropiles (a) MC1 and (b) MC2.

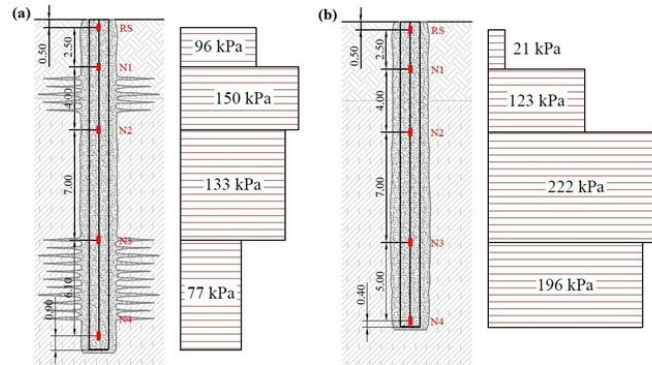


Figure 13. Maximum skin friction along depth for micropiles (a) MC1 and (b) MC2.

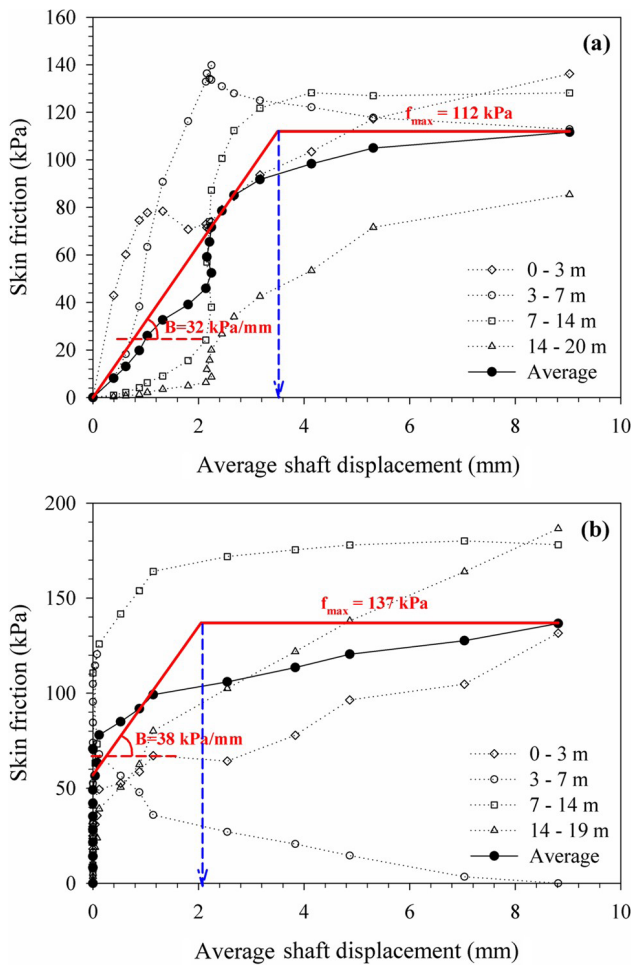


Figure 14. Average maximum unitary friction vs average shaft displacement for micropiles (a) MC1 and (b) MC2.

2005, 2007; Albuquerque & Carvalho, 2017; Fiscina et al., 2021). The upper stiffness bound varies between 45 and 25 kPa/mm and the lower bound between 25 and 5 kPa/mm, with the trend line varying between 35 and 15 kPa/mm. Traditional bored piles fully mobilized the skin friction for shaft displacements inferior to 1 mm, whereas root piles developed displacements close to 6 mm to mobilize the

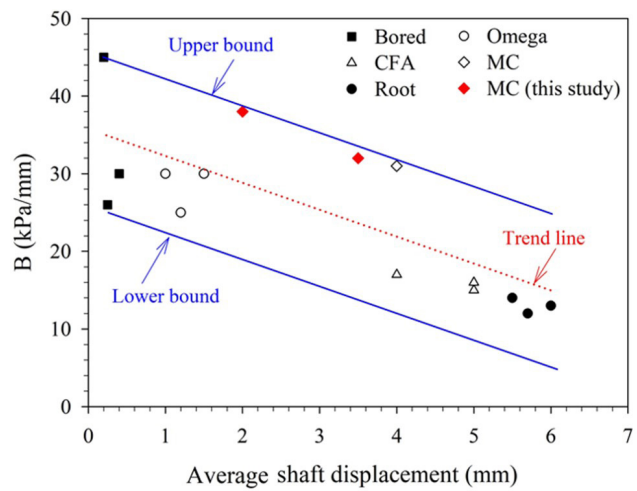


Figure 15. Variation in B parameter of piles performed at ES I.

maximum skin friction. The micropiles presented in this study were close to the upper stiffness bound with displacements between 2 mm and 4 mm.

Figure 16 presents the maximum skin friction variation for the piles performed at the ES I and the ES III. The maximum skin friction for the first layer of ES I (silty clay / depth of 0 to 5m / $N_{SPT} = 4$ blows) had an average value of 56 kPa (coefficient of variation = 34%). However, the same layer in the ES III – adding the results from Fiscina et al. (2021) for a micropile (MC 0) with $\phi = 0.3$ m and $L = 17$ m – shows higher maximum skin friction in the first layer compared with that obtained for the piles installed at the ES I, with an average value of 101 kPa (CV = 22%). This value is 80% higher than the mobilized skin friction values from the ES1, showing that the construction process influences the performance of the pile. The first layer is a tropical lateritic soil, which, despite presenting low resistance values in the CPTu and SPT tests, results in higher skin friction due to the internal cementation inherit from this type of soil. This phenomenon was also observed by Décourt (2008), Schulze (2013) and Albuquerque et al. (2007) with piles performed in the same type of soil.

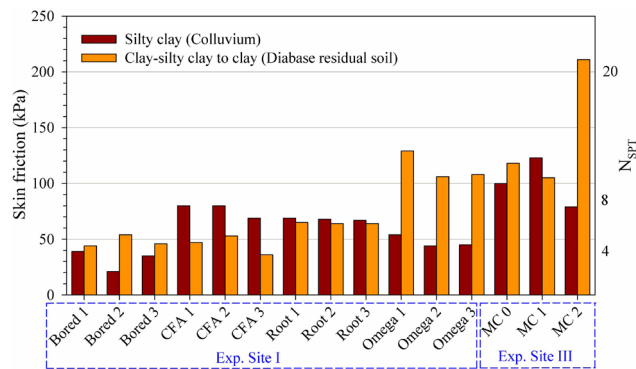


Figure 16. Skin friction variation for local soil profile.

Regarding the second representative soil layer, the piles installed in the ES I exhibit a maximum length of 12 m, with 7 m embedded in the residual soil layer with $N_{SPT,ave} = 8$ blows, whereas in ES III, the micropiles vary between 16 and 21 m in length, with 11 to 16 m embedded in that same soil layer but with an $N_{SPT,ave} = 20$ blows, which prevents a quantitative comparison. However, it was observed that, excluding the micropile MC2, the behavior was similar to that of omega piles from the ES I, with friction values around 110 kPa (114 kPa).

5. Conclusions

This work presented a new post-grouted micropile type installed in a tropical soil. Two instrumented static load-maintained tests were performed to verify its behavior and design parameters, and results were compared with other types of piles installed in the same subsoil profile. Main conclusions from results are as follows:

- The FHWA (2005) method of estimating the ultimate geotechnical pile capacity best fitted with the values from the load tests. The authors recommend using the average values of q_s suggested by the FHWA (2005) for this type of soil (tropical lateritic soil) and micropiles aiming to estimate the geotechnical capacity for future designs. The Bustamante & Doix (1985) method showed that the volume and injection correction parameters would be inadequate for the studied micropiles and for the local condition, thus requiring further studies. In addition, pile tip resistance can be ignored for these types of piles. The Lizzi (1985) method, despite being developed for root piles and showing results outside the $\pm 20\%$ range, proved to be a usable method. However, further studies are required to propose a correction coefficient for this method.

- Comparing the maximum skin friction calculated from the method suggested by the FHWA (2005) and the values obtained from the load tests, the calculated values are lower, especially in the layers up to 7 m of depth. This suggests that this specific

layer contain additional resistance due to its natural cementation (typical of lateritic soils).

- The instrumentation technique used was efficient. For stresses above 25 MPa, the instrumentation presents a creep response, indicating that the load vs deformation mechanism stops being proportional for values beyond that point, which should be avoided in load tests. The incremental stiffness method proposed by Komurka & Moghaddam (2020) is appropriate, considering that the behavior is non-linear and the transversal section is irregular;
- The deformation modules were inferior to those obtained for concrete piles, which was expected due to the use of neat cement grout instead of concrete (Fiscina et al., 2021). The loss of stiffness in part of the shaft of one of the piles suggests the occurrence of the debonding effect caused by the low resistance of the neat cement grout, which was lower than the values suggested by the FHWA (2005) standards.
- The piles showed that the maximum skin friction was mobilized for average shaft displacements of around 1% of the pile diameter (300 mm), similar to the behavior of other types of piles performed at Unicamp, which work mostly by friction. The stiffness of the micropiles showed higher values compared to the other piles installed at Unicamp, indicating that the installation process improves the friction performance.
- The new micropile construction methodology proved to be promising in terms of improving the shaft resistance, showing average skin friction above 110 kPa, which is 1.3 to 3.8 times higher than the average friction observed in other types of piles performed in similar ground conditions. However, there was no effective gain of resistance by lateral friction due to the post-grouting treatment, which indicates that only the injection of the annulus sheath is indicative of improvement in the performance by friction.

Acknowledgements

The authors thank the University of Campinas (Unicamp) and INCOTEP for the support given to build the experimental site and the micropiles. We also thank Coordenação de Aperfeiçoamento de Pessoal de Nível Superior (CAPES) for the study grants to the graduate students involved in this research.

Declaration of interest

The authors have no conflicts of interest to declare. All co-authors have observed and affirmed the contents of the paper and there is no financial interest to report.

Authors' contributions

Joaquim Ribeiro Castro Neto: conceptualization, data curation, investigation, methodology, writing – original draft. Paulo José Rocha de Albuquerque: conceptualization, methodology, supervision, validation, project administration, writing – review and editing. Yuri Barbosa: investigation, methodology, writing – review and editing. Luiz Felipe Goulart Fiscina: investigation, methodology, writing – review and editing.

List of symbols

q_c	Measured cone resistance
f_s	Unit sleeve friction resistance
API	American Petroleum Institute
B	Stiffness
CPTu	Cone Penetration Test
CV	Coefficient of variation
ES I	Experimental Site I
ES III	Experimental Site III
MC 1	Micropile 1
MC 2	Micropile 2
N_{SPT}	Standard Penetration Test blows count
Q_{est}	Estimate Load by Method
Q_{SMLT}	Load Test Load Measured
SPT	Standard Penetration Test
SR	Reference Section

References

- ABNTNBR 12131. (2006). *Estacas: prova de carga estática: método de ensaio*. ABNT - Associação Brasileira de Normas Técnicas, Rio de Janeiro, RJ (in Portuguese).
- Albuquerque, P.J.R. (2001). *Estacas escavadas, hélice contínua e ômega: estudo do comportamento à compressão em solo residual de diabásio, através de provas de carga instrumentadas em profundidade* [Doctoral thesis]. Universidade de São Paulo (in Portuguese). <https://doi.org/10.11606/T.23.2019.tde-07082019-100623>.
- Albuquerque, P.J.R., Carvalho, D., Alledi, C.T.D.B., & Polido, U.F. (2007). Behavior of instrumented continuous flight auger piles in sedimentary and residual soils. In *Proceedings of the 13th Panamerican Conference on Soil Mechanics and Geotechnical Engineering* (pp. 1-6). Venezuelan Geotechnical Society.
- Albuquerque, P.J.R., Freitas Neto, O., & Garcia, J.R. (2014). Behavior of instrumented omega pile in porous soil. *Advanced Materials Research*, 1030, 732-735. <http://dx.doi.org/10.4028/www.scientific.net/AMR.1030-1032.732>.
- Albuquerque, P.J.R., & Carvalho, D. (2017). Effect of second loading on the instrumented continuous flight auger concrete pile on porous soil. *Key Engineering Materials*, 753, 285-289. <http://dx.doi.org/10.4028/www.scientific.net/KEM.753.285>.
- Albuquerque, P.J.R., Carvalho, D., & Massad, F. (2005). Bored, continuous flight auger and omega instrumented piles: Behavior under compression. In *Proceedings of the 16th International Conference on Soil Mechanics and Geotechnical Engineering* (pp. 339-345). IOS Press.
- Allen, C., Jesús, G., Donald, B., & Tom, A. (2004). Micropiles: recente advances and future trends. In *Proceedings of the Current Practices and Future Trends in Deep Foundations* (pp. 140-415), Los Angeles. ASCE Geotechnical Special Publication. [https://doi.org/doi:10.1061/40743\(142\)9](https://doi.org/doi:10.1061/40743(142)9).
- Aoki, N. (1976). *Considerações sobre a capacidade de carga de estacas isoladas*. Rio de Janeiro: Universidade Gama Filho, 44p.
- Bustamante, M., & Doix, B. (1985). Une méthode pour le calcul des tirants et des micropieux injectés. *Bulletin de Liaison des Laboratoires des Ponts et Chaussées*, 140, 75-92 (in French).
- Castro Neto, J.R. (2021). *Estaca injetada instrumentada tipo Incopile: avaliação do comportamento à compressão em solo tropical da região de Campinas/SP* [Master's dissertation]. Universidade Estadual de Campinas (in Portuguese). Retrieved in June 21, 2022, from <https://hdl.handle.net/20.500.12733/1641142>
- Choi, C., & Cho, S.D. (2010). Field verification study for micropile load capacity. In *Proceedings of the 10th International Workshop on Micropiles* (pp. 1-10), Washington, DC.
- Décourt, L. (2008). Loading tests: interpretation and prediction of their results. In *Proceedings of the Research to Practice in Geotechnical Engineering* (pp. 452-470). New Orleans: ASCE. [http://dx.doi.org/10.1061/40962\(325\)16](http://dx.doi.org/10.1061/40962(325)16).
- Dias, T.G.S., & Bezuijen, A. (2018). Load-transfer method for piles under axial loading and unloading. *Journal of Geotechnical and Geoenvironmental Engineering*, 144(1), 04017096. [http://dx.doi.org/10.1061/\(ASCE\)GT.1943-5606.0001808](http://dx.doi.org/10.1061/(ASCE)GT.1943-5606.0001808).
- Ebrahimian, B., & Movahed, V. (2017). Application of an evolutionary-based approach in evaluating pile bearing capacity using CPT results. *Ships and Offshore Structures*, 12(7), 937-953. <http://dx.doi.org/10.1080/17445302.2015.1116243>.
- Eid, M., Hefny, A., Sorour, T., & Zagh, Y. (2018). Full-scale well instrumented large diameter bored pile load test in multi layered soil: a case study of damietta port new grain silos project. *International Journal of Current Engineering and Technology*, 8(01), 85-98. <http://dx.doi.org/10.14741/ijcet.v8i01.10895>.
- Fattah, M.Y., Al-Omari, R.R., & Fadhil, S.H. (2020). Load sharing and behavior of single pile embedded in unsaturated swelling soil. *European Journal of Environmental and Civil Engineering*, 24(12), 1967-1992. <http://dx.doi.org/10.1080/19648189.2018.1495105>.

- Fellenius, B.H. (1989). Tangent modulus of piles determined from strain data. In *Proceedings of the ASCE Geotechnical Engineering Division Foundation Congress* (pp. 500-510), Evanston. ASCE.
- Fellenius, B.H. (2001). From strain measurements to load in an instrumented pile. *Geotechnical News Magazine*, 19(1), 35-38.
- Fellenius, B.H. (2021). *Basics of foundation design*. (Electronic Edition). Retrieved in June 21, 2022, from <https://www.fellenius.net>
- FHWA NHI-05-039. (2005). *Micropile design and construction*. FHWA - Federal Highway Administration, U. S. Department of Transportation, Washington, DC.
- Finno, R.J., Scherer, S.D., Paineau, B., & Roboski, J. (2002). Load transfer characteristics of micropiles in dolomite. In *Proceedings of the Deep Foundations 2002: An International Perspective on Theory, Design, Construction, and Performance* (pp. 1038-1053), Orlando. ASCE. [http://dx.doi.org/10.1061/40601\(256\)73](http://dx.doi.org/10.1061/40601(256)73).
- Fiscina, L.F.G. (2020). *On the interpretation of the failure mechanism of instrumented post-grouted micropiles submitted to compression and tensile axial loads in diabase soil* [Master's dissertation]. Universidade Estadual de Campinas. Retrieved in June 21, 2022, from <https://hdl.handle.net/20.500.12733/1640794>
- Fiscina, L.F.G., Barbosa, Y., Albuquerque, P.J.R., & Carvalho, D. (2021). Field study on axial behavior of instrumented post-grouted steel pipe micropiles in tropical lateritic soil. *Innovative Infrastructure Solutions*, 6(2), 1-17. <http://dx.doi.org/10.1007/s41062-020-00411-x>.
- Freitas Neto, O., Cunha, R.P., Albuquerque, P.J.R., Garcia, J.R., & Santos Júnior, O.F.D. (2020). Experimental and numerical analyses of a deep foundation containing a single defective pile. *Latin American Journal of Solids and Structures*, 17(3), 1-15. <http://dx.doi.org/10.1590/1679-78255827>.
- Gomez, J., Cadden, A., & Bruce, D.A. (2003). Micropiles founded in rock: development and evolution of bond stress under repeated loading. In *Proceedings of 12th Panamerican Conference on Soil Mechanics and Geotechnical Engineering* (pp. 1911-1916), Cambridge. Verlag Glückauf GMBH.
- Han, F., Salgado, R., Prezzi, M., & Lim, J. (2017). Shaft and base resistance of non-displacement piles in sand. *Computers and Geotechnics*, 83, 184-197. <http://dx.doi.org/10.1016/j.compgeo.2016.11.006>.
- Holman, T.P., & Barkauskas, B.D. (2007). Mechanics of micropile performance from instrumented load tests. In *Proceedings of 7th FMGM 2007: Field Measurements in Geomechanics* (pp. 1-14). Boston: ASCE. [http://dx.doi.org/10.1061/40940\(307\)8](http://dx.doi.org/10.1061/40940(307)8).
- Jeong, S., Kim, D., & Park, J. (2021). Empirical bearing capacity formula for steel pipe prebored and precast piles based on field tests. *International Journal of Geomechanics*, 21(9), 04021165. [http://dx.doi.org/10.1061/\(ASCE\)GM.1943-5622.0002112](http://dx.doi.org/10.1061/(ASCE)GM.1943-5622.0002112).
- Khanmohammadi, M., & Fakharian, K. (2019). Numerical modelling of pile installation and set-up effects on pile shaft capacity. *International Journal of Geotechnical Engineering*, 13(5), 484-498. <http://dx.doi.org/10.1080/19386362.2017.1368185>.
- Kim, D., Jeong, S., & Park, J. (2020). Analysis on shaft resistance of the steel pipe prebored and precast piles based on field load-transfer curves and finite element method. *Soil and Foundation*, 60(2), 478-495. <http://dx.doi.org/10.1016/j.sandf.2020.03.011>.
- Ko, J., Seo, H., Kim, S., & Kim, S. (2018). Numerical analysis for mechanical behavior of pipe pile utilized for compressed air energy storage. In *Proceedings of the IFCEE 2018* (pp. 715-723). Orlando: ASCE. <http://dx.doi.org/10.1061/9780784481578.068>.
- Komurka, V.E., & Moghaddam, R.B. (2020). The incremental rigidity method: more direct conversion of strain to internal force in an instrumented static loading test. In *Proceedings of the Geo-Congress 2020* (pp. 124-134), Minneapolis. ASCE. <http://dx.doi.org/10.1061/9780784482780.013>.
- Laister, E., Albuquerque, P.J.R., Camarini, G., & Carvalho, D. (2014). The influence of cement and water to cement ratio on capillary absorption of root-pile mortars. *Soils and Rocks*, 37(2), 171-176. <http://dx.doi.org/10.28927/SR.372171>.
- Lizzi, F. (1985). The pali radice (root piles): a state-of-the-art report. In *Proceedings of the Symposium on Recent Developments in Ground Improvement Techniques* (pp. 417-450). Bangkok: Balkema.
- Loukidis, D., & Salgado, R. (2008). Analysis of the shaft resistance of non-displacement piles in sand. *Geotechnique*, 58(4), 283-296. <http://dx.doi.org/10.1680/geot.2008.58.4.283>.
- Mendoza, C.C., Caicedo, B., & Cunha, R. (2017). Determination of vertical bearing capacity of pile foundation systems in tropical soils with uncertain and highly variable properties. *Journal of Performance of Constructed Facilities*, 31(1), 04016068. [http://dx.doi.org/10.1061/\(ASCE\)CF.1943-5509.0000918](http://dx.doi.org/10.1061/(ASCE)CF.1943-5509.0000918).
- Meyer, Z., & Żarkiewicz, K. (2018). Skin and toe resistance mobilisation of pile during laboratory static load test. *Studia Geotechnica et Mechanica*, 40(1), 1-5. <http://dx.doi.org/10.2478/sgem-2018-0001>.
- Moshfeghi, S., & Eslami, A. (2018). Study on pile ultimate capacity criteria and CPT-based direct methods. *International Journal of Geotechnical Engineering*, 12(1), 28-39. <http://dx.doi.org/10.1080/19386362.2016.1244150>.
- Niazi, F.S., & Mayne, P.W. (2013). Cone penetration test based direct methods for evaluating static axial capacity of single piles. *Geotechnical and Geological Engineering*, 31(4), 979-1009. <http://dx.doi.org/10.1007/s10706-013-9662-2>.
- Ong, Y.H., Toh, C.T., Chee, S.K., & Mohamad, H. (2021). Bored piles in tropical soils and rocks: shaft and base resistances, t-z and q-w models. *Geotechnical Engineering*, 174(2), 193-224. <http://dx.doi.org/10.1680/jgeen.19.00106>.
- Park, J.H., Kim, D., & Chung, C.K. (2012). Implementation of Bayesian theory on LRFD of axially loaded driven

- piles. *Computers and Geotechnics*, 42, 73-80. <http://dx.doi.org/10.1016/j.compgeo.2012.01.002>.
- Russo, G. (2004). Full-scale load tests on instrumented micropiles. *Geotechnical Engineering*, 157(3), 127-135. <http://dx.doi.org/10.1680/geng.2004.157.3.127>.
- Schulze, T. (2013). *Análise da capacidade de carga de estaca escavada instrumentada de pequeno diâmetro por meio de métodos semi-empíricos* [Master's dissertation]. Universidade Estadual de Campinas (in Portuguese). <http://dx.doi.org/10.47749/T/UNICAMP.2013.909385>.
- Song, C.R., Bekele, B., Silvey, A., Lindemann, M., & Ripa, L. (2020). Piezocone/cone penetration test-based pile capacity analysis: calibration, evaluation, and implication of geological conditions. *International Journal of Geotechnical Engineering*, 16(3), 343-356. <http://dx.doi.org/10.1080/19386362.2020.1778214>.
- Titi, H.H., & Abu-Farsakh, M.Y. (1999). *Evaluation of bearing capacity of piles from cone penetration test data*. Retrieved in June 21, 2022, from <https://rosap.nrl.bts.gov/view/dot/22095>
- Van der Veen, C. (1953). The bearing capacity of pile. In *Proceedings of the International Conference on Soil Mechanics and Foundation Engineering* (pp. 84-90). Zürich: ICOSOMEF.
- Wada, A. (2004). Skin friction and pile design. In *Proceedings of the 5th International Conference on Case Histories in Geotechnical Engineering* (pp. 1-7). New York: University of Missouri-Rolla. Retrieved in June 21, 2022, from <https://scholarsmine.mst.edu/icchge/5icchge/session01/14>
- Wan, Z.H., Dai, G.L., & Gong, W.M. (2019). Field study on post-grouting effects of cast-in-place bored piles in extra-thick fine sand layers. *Acta Geotechnica*, 14(5), 1357-1377. <http://dx.doi.org/10.1007/s11440-018-0741-7>.
- Wrana, B. (2015). Pile load capacity: calculation methods. *Studia Geotechnica et Mechanica*, 37(4), 83-93. <http://dx.doi.org/10.1515/sgem-2015-0048>.